Thermal Model of Cylindrical and Prismatic Lithium-Ion Cells

Article *in* Journal of The Electrochemical Society · July 2001

DOI: 10.1149/1.1377592

4 authors, including:

Timothy Hatchard
Dalhousie University
58 PUBLICATIONS **2,734** CITATIONS

SEE PROFILE

Journal of The Electrochemical Society, **148** (7) A755-A761 (2001)
0013-4651/2001/148(7)/A755/7/$7.00 © The Electrochemical Society, Inc.

Thermal Model of Cylindrical and Prismatic Lithium-Ion Cells

T. D. Hatchard,[a,*] D. D. MacNeil,[b,*] A. Basu,[c] and J. R. Dahn[d,,z]**

[a]*Department of Physics,* [b]*Department of Chemistry,* [c]*Department of Computer Science, and* [d]*Departments of Physics and Chemistry, Dalhousie University, Halifax, Nova Scotia B3H 3J5, Canada*

Oven exposure testing is a standard benchmark that Li-ion cells must pass in order to be approved for sale by regulating bodies. In order to test the safety of new cell designs or electrode materials, manufacturers must make small test batches of cells. This can be both costly and time consuming. Using reaction kinetics that have been developed for electrode materials with electrolyte exposed to high temperature, and thermal properties of cells from the literature, a predictive model for oven exposure testing has been developed. The model predictions are compared to oven exposure test results for E-One/Moli Energy, Canada, 18650 $LiCoO_2$/graphite cells and shown to be in good agreement. The model can predict the response of new cell sizes and electrode materials to oven exposure testing without actually producing any cells. This is illustrated with a number of examples: (*i*) increasing the specific surface area of the graphite electrode; (*ii*) using $LiMn_2O_4$ or other cathode substitutes instead of $LiCoO_2$; (*iii*) varying the diameter of cylindrical cells; and (*iv*) varying the thickness of prismatic cells.
 [DOI: 10.1149/1.1377592]

Manuscript submitted September 25, 2000; revised manuscript received February 20, 2001. Available electronically June 6, 2001.

Lithium-ion batteries are the state-of-the-art power sources for portable electronics. They combine excellent cycle life, no memory effect, and high energy density. There is a constant desire to improve the capacity and cycle life of these cells, and as a result battery manufacturers are always looking to develop new and improved electrode materials. These new materials, when used in mass produced cells, would also have to meet regulations and industry standards regarding the safety of the cells. One of the most important safety considerations for lithium-ion cells is their thermal stability under various abuses such as exposure to heat, nail penetration, external short circuit, crushing, and so on. In order for a manufacturer to evaluate the safety of a new electrode material (or even a new electrolyte with existing electrode materials) it would be necessary to produce a small batch of cells (on the order of 100) and perform tests on them under abuse conditions. This would require a substantial amount of the new material to be made.

A technique has been developed to determine ''power functions'' for carbon and cobalt electrodes in electrolyte.[1-3] The power functions are kinetic triplets (reaction model, frequency factor, and activation energy) that describe the kinetics of the reactions between electrolyte and electrode material. The technique uses accelerating rate calorimetry (ARC) and differential scanning calorimetry (DSC) tests to obtain a small number of reaction kinetic parameters. This technique requires little material (for example, 10 g of electrode material is more than enough[4]) to be tested. The power functions give the heat produced by chemical reactions between a unit mass of electrode material and electrolyte at a given temperature per unit time. Also available in the literature are values for thermal properties of lithium-ion cells such as average heat capacity and average thermal conductivity of the jelly roll material (electrodes, separator, and current collectors).[5,6] Using the power functions and thermal properties of cells, it is possible to create a mathematical model that describes the heat production and flow within a lithium-ion cell. A manufacturer could then use this model to predict the thermal behavior of a cell with a new electrode material or electrolyte without having to produce an expensive test batch of cells.

Description of the Model

The first step in building the model was to determine if a simple numeric model would provide accurate results for the heat flow in the cell. It was decided to target a certain cell geometry for the purposes of building the model and testing accuracy. It would then be generalized to other sizes and shapes after the model was perfected. The shape chosen was a standard 18650 cylindrical cell. The cylinder was considered as a series of N concentric rings of equal width. Heat flow between the rings would then be determined by their width, thermal conductivity, and the temperature difference between them. Newton's law of cooling was selected to describe heat flow at the surface. Axial heat flow was ignored to simplify the model. This simplification is addressed further later.

The first case tested was a solid cylinder of constant composition, at a certain starting temperature, in surroundings having a temperature T_w with no heat produced within the cylinder. The temperature change, ΔT, in each ring during an infinitesimal time interval, Δt, is given by

$$\Delta T_i = \left[\frac{k(T_{i+1} - T_i)2\pi r_i}{(r_{i+1} - r_i)} + \frac{k(T_{i-1} - T_i)2\pi r_{i-1}}{(r_i - r_{i-1})} \right] \cdot \frac{\Delta t}{C\rho(\pi r_i^2 - \pi r_{i-1}^2)} \quad [1]$$

$$\Delta T_N = \left[\frac{k(T_N - T_{N-1})2\pi r_{N-1}}{(r_N - r_{N-1})} + (T_w - T_N)h2\pi r_N \right] \cdot \frac{\Delta t}{C\rho(\pi r_N^2 - \pi r_{N-1}^2)} \quad [2]$$

ΔT_i is the temperature change of the ith ring and ΔT_N is the temperature change of the outermost ring in the time Δt. The outer radius of the ith ring is r_i, k is the thermal conductivity of the cylinder material, Δt is the time step used (typically 0.001 s for solid, homogeneous cylinders), C is the specific heat capacity of the cylinder material, ρ is the density of the material, and h is the heat-transfer coefficient of the cylinder. The first term of the equations calculates the heat flowing into the ring per unit time from the neighboring inner ring, and the second term calculates the heat flowing into the ring per unit time from the neighboring outer ring (or environment). This model was coded in Fortran with the temperature of each ring being tracked as a function of time.

There is an analytical solution for this situation that gives the temperature in the cylinder as a function of time and radius.[7] This was also coded in Fortran to be used as a check of the numerical model. It was also possible to check this model against experiment (described later).

The second case tested was a solid cylinder of constant composition at a certain starting temperature, in surroundings at a constant temperature, T_w, with a constant heat per unit time per unit volume

* Electrochemical Society Student Member.
** Electrochemical Society Active Member.
z E-mail: jeff.dahn@dal.ca

produced within the cylinder. The temperature change in each ring is again given by Ref. 1 and 2 except there is now a third term in the square brackets of those equations

$$P_i[\pi(r_i^2 - r_{i-1}^2)] \quad [3]$$

P_i is a constant heat generation rate per unit volume produced in the ring, and the rest gives the volume of the ring (effectively, an infinite cylinder is being modeled so the calculations give results per unit length). This was also coded in Fortran with the temperature of each ring being tracked as a function of time. There is also an analytical solution for this case that gives the temperature in the cylinder as a function of time and radius.[7] Again, this was coded in Fortran to provide a check of the numerical model, although no experimental check was made for this case.

The final test was to build the model of an actual 18650 lithium-ion cell. The same N-ring model was used, but this time it was not possible to check against an analytical solution. The temperature in the *i*th ring was calculated as in the previous case, except the heat generation rate, P_i, is no longer a constant. For the carbon electrode the heat generation rate is given by

$$P = H_1 A_1 x_f^n \exp\left(\frac{-E_1}{K_b T}\right) + H_2 A_2 x_i \exp\left(\frac{-z}{z_o}\right)\exp\left(\frac{-E_2}{K_b T}\right) \quad [4]$$

where the two terms are for two separate reactions at the carbon electrode. H_1 and H_2 are the total amounts of heat that can be produced by each reaction per unit mass of reactant, A_1 and A_2 are frequency factors, and E_1 and E_2 are activation energies for the reactions. This gives the heat generation rate per unit mass of electrode material. The parameters x_f, x_i, and z are functions of the type of carbon used and how they are charged as described in Ref. 1. x_f is the amount of lithium-containing metastable species in the solid electrolyte interphase (SEI, measured relative to x in Li_xC_6), x_i is the amount of lithium intercalated within the carbon, and z is a dimensionless measure of the SEI thickness.[1] The changes in the parameters are tracked as well as the temperature changes. These are as follows

$$\Delta x_f = -A_1 x_f^n \exp\left(\frac{-E_1}{K_b T}\right)\Delta t \quad [5]$$

$$\Delta x_i = -A_2 x_i \exp\left(\frac{-z}{z_o}\right)\exp\left(\frac{-E_2}{K_b T}\right)\Delta t \quad [6]$$

$$\Delta z = A_2 x_i \exp\left(\frac{-z}{z_o}\right)\exp\left(\frac{-E_2}{K_b T}\right)\Delta t \quad [7]$$

For the cobalt electrode, the heat generation rate is given by

$$P = HA \exp\left(\frac{-E}{K_b T}\right)\alpha^m(1-\alpha)^n[-\ln(1-\alpha)]^p \quad [8]$$

or

$$P = H\frac{\partial \alpha}{\partial t} \quad [9]$$

Here, H is again the total heat produced by the reaction per unit mass, A is a frequency factor, E the activation energy, and α is the fractional degree of conversion. This equation also gives the heat generation rate per unit mass. The exponents m, n, and p are selected based on the type of kinetics that govern the reaction. They can be chosen based on a best fit of data or to correspond to previously studied kinetic models in the literature.[3] A choice of m = 1, n = 1, and p = 0 corresponds to autocatalytic kinetics, as has been found to fit the first exotherm of the $LiCoO_2$/electrolyte reaction fairly well.[2,3]

The outer ring was treated differently, with the assumption being made that half the ring was jellyroll material and half was the cell can. The value of h, the heat-transfer coefficient, depends not only on the geometry of the cell and the surrounding medium, but also on the material of the surface. An appropriate value of h is needed depending on whether or not the cell is labeled and on what type of label it has.[8]

This model was also coded in Fortran. The code not only kept track of temperature in each ring but also the parameters for the power functions. As can be seen, the number of parameters for the final model is quite large. It was desired to have a graphical interface and an easy-to-use environment for the model. The final Fortran code was transposed to C++, and an application developed using Visual C++. This application allows the user to easily adjust the numerous parameters and then perform a calculation to see what the results would be for a full-sized cell. Also included are functions that allow calculations of ARC and DSC results for electrode materials. This can simplify fine-tuning of parameters until calculated ARC or DSC curves match collected data. The calculations for a full-sized cell should then produce a close approximation to the performance of a real cell in an oven exposure test.

An option to calculate oven exposure profiles for a prismatic cell was also included in the model. The calculations were similar to those for a cylinder, except the prismatics were divided into N layers, with heat flow through the edges ignored. If the cells are long and wide and kept relatively thin, then the bulk of the surface area is in the two large faces, with the edges making a minimal contribution. The temperature change in each layer is given by

$$\Delta T_i = \left[\frac{k(T_{i+1} - T_i)LW}{B/N} + \frac{k(T_{i-1} - T_i)LW}{B/N} + P_i[LW(B/N)]\right] \cdot \frac{\Delta t}{C\rho LW(B/N)} \quad [10]$$

Here L and W represent the length and width of the cell, N is the number of layers, and B is the cell height or thickness. All other variables are the same as in Eq. 1 and 2.

Experimental

In order to provide a check of the accuracy of the computer models, it was necessary to collect data for the situations that the models described. For the case of the cylinder with no internally produced heat, cylinders were made with the dimensions of an 18650 lithium-ion cell. Cylinders were made from aluminum, brass, and stainless steel. Values are readily available for the thermal properties of these metals,[9] although the heat-transfer coefficient was found via the method described in Ref. 8. A thermocouple was ''banded'' to the metal cylinder with four or five pieces of fine wire. The thermocouple was then covered by a small amount of Wakefield's thermal compound and then insulated from outside temperature influences by a small amount of glass wool. The cylinder was then lowered into a VWR Scientific gravity convection oven preheated to a set temperature. The oven was kept at a constant temperature, and temperature *vs.* time data was recorded for the outside edge of the cylinder. This was repeated for each of the three different cylinders.

In order to check the accuracy of the model for the interior of the cylinder, a 2 mm-diam hole was drilled down the center axis of the stainless steel and aluminum cylinders. These cylinders were also placed in the oven in the manner described, but this time there was also a thermocouple inserted in the central axis along with some thermal compound to ensure good thermal contact. The top of the hole was stuffed with glass wool to insulate against heating of the cylinder from the inside out. Temperature *vs.* time data were collected for both the edge of the cylinder and the central axis.

In order to assess the importance of axial heat flow, some tests were also performed with the ends of the cylinder insulated. Blocks of foam insulation were fixed to the ends of the cylinders in order to

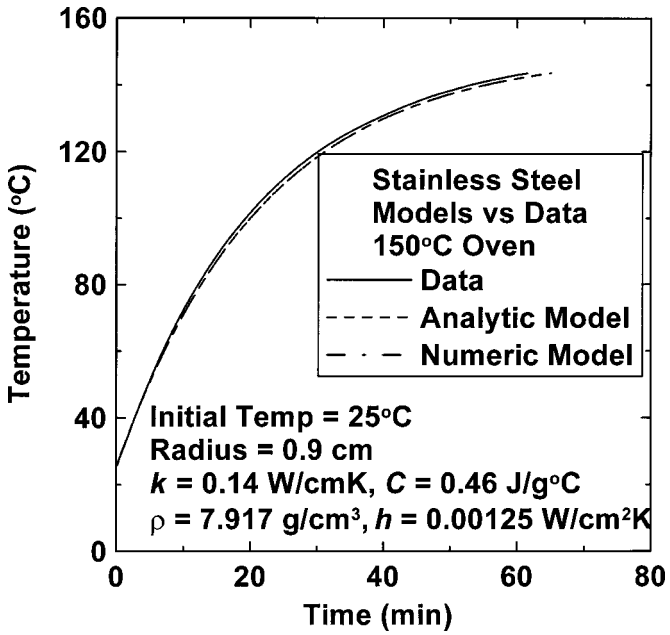

Figure 1. A comparison of model predictions to actual data for a solid stainless steel cylinder: (—) oven data, (– – –) model predictions.

minimize the heat flow from end to end, and ensure that the majority of the heat transferred to the cylinder came from the side (in the radial direction). These tests had to be performed at somewhat lower temperature to keep the insulation from melting.

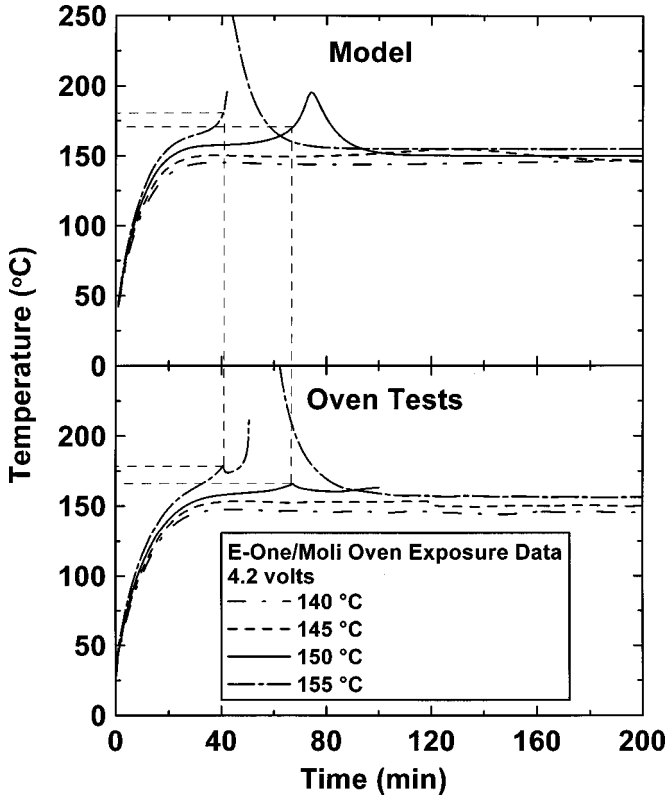

Figure 2. A comparison of oven exposure test results to model predictions: (top) model predictions and (bottom) oven test results for 18650 E-One/Moli Energy cells charged to 4.2 V.

Table I. Standard model parameters used to describe E-One/Moli Energy $LiCoO_2$/graphite chemistry.

Parameter	Value
Cathode frequency factor, γ	4×10^{13} (min)
Cathode activation energy, E_a	1.27 (eV)
Cathode α_o	0.04 (unitless)
Cathode m	1 (exponent)
Cathode n	1 (exponent)
Cathode p	0 (exponent)
Cathode H	314 (J/g)
Anode SEI frequency factor, A_1	1×10^{17} (min)
Anode intercalated lithium frequency factor, A_2	1.5×10^{15} (min)
Anode SEI activation energy, E_1	1.4 (eV)
Anode intercalated lithium activation energy, E_2	1.4 (eV)
Anode x_{fo}	0.15 (dimensionless)
Anode x_{io}	0.75 (dimensionless)
Anode z_o	0.033 (dimensionless)
Anode n	1 (exponent)
Anode SEI H	257 (J/g)
Anode intercalated lithium H	1714 (J/g)
Carbon mass	
(Cylindrical, 18650)	6 (g)
(Thin prismatic, 3.5 × 6.2 × 0.36 cm)	1.7 (g)
(Thick prismatic, 3.5 × 6.2 × 1.5 cm)	7.2 (g)
$LiCoO_2$ mass	
(Cylindrical, 18650)	12 (g)
(Thin Prismatic, 3.5 × 6.2 × 0.36 cm)	4.1 (g)
(Thick Prismatic, 3.5 × 6.2 × 1.5 cm)	17 (g)
Start temperature	28 (°C)
Average cell specific heat, C[8]	0.83 (J/g K)
Average jelly roll radial thermal conductivity[5]	0.034 (W/cm K)
Average jelly roll density (cylindrical)	2.58 (g/cc)
Average density (prismatic)	1.70 (g/cc)
Can density[9]	7.917 (g/cc)
Can specific heat[9]	0.46 (J/g K)
Surface emissivity	0.80 (dimensionless)
(matches that of E-one/Moli label[8])	
Can thermal conductivity[9]	0.14 (W/cm K)
Length (cylindrical, 18650)	6.5 (cm)
Length (prismatic)	6.2 (cm)
Radius (cylindrical)	0.9 (cm)
Width (prismatic)	3.5 (cm)
Thickness (prismatic)	Thin 0.36 (cm)
	Thick 1.5 (cm)

To test the completed thermal model, tests were also performed on lithium-ion cells. These cells were E-One/Moli Energy ICR18650 (18 mm diam, 65 mm length) 1.65 Ah cobalt cells. Tests were performed on cells at various states of charge (4.1, 4.2, and 4.3 V), with and without manufacturer's labels and at oven temperatures ranging from 130 to 160°C. These tests were performed in the same way as the tests on solid cylinders (except no holes were drilled down the center), and temperature *vs.* time data were recorded for each. Electrode powders and electrolyte were also provided by the manufacturer, and the parameters for the power functions were obtained as described in Ref. 1-3.

Results and Discussion

All the tests performed to check the ability of the simple numeric model (with no heat generated within the cylinder) to produce accurate results showed excellent agreement with each other and with data. In the situations where the numeric model was compared with an analytic solution, the two produced identical results. When the numeric model or analytic solution was compared with collected data, the results were nearly identical, differing by less than five percent. An example is shown in Fig. 1, with the parameters used listed in the figure. The samples placed in the oven would heat slightly faster than predicted because they gained heat through the ends of the cylinder which were ignored in the model. Insulating the ends of the cylinder to minimize axial heat flow brought the differ-

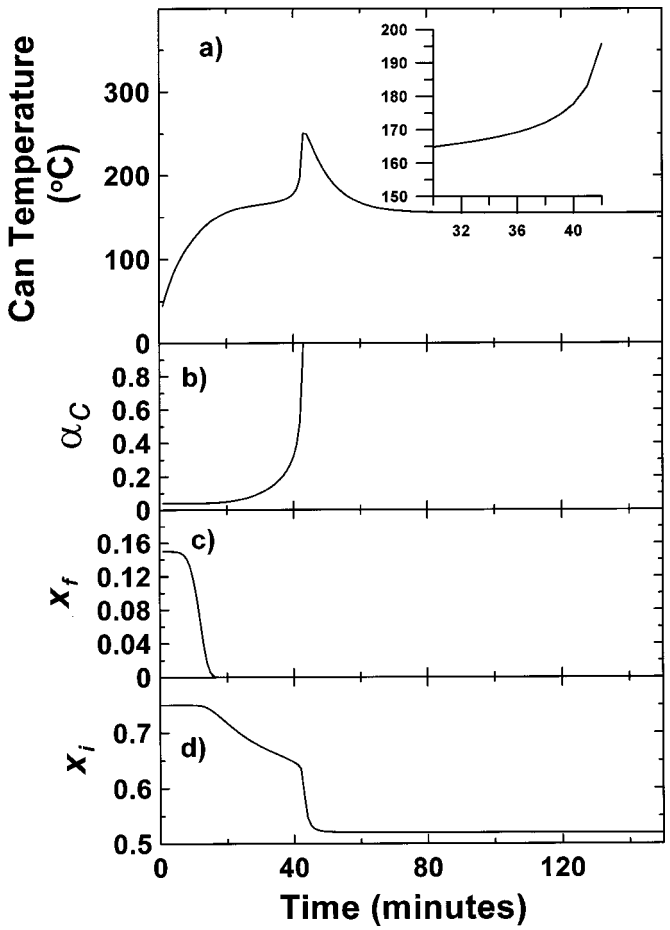

Figure 3. Tracking the changes in parameters during an oven exposure test: (a) surface temperature of the cell, (b) fractional degree of conversion for the cathode, (c) decomposition of SEI layer, and (d) reaction of intercalated lithium at the anode.

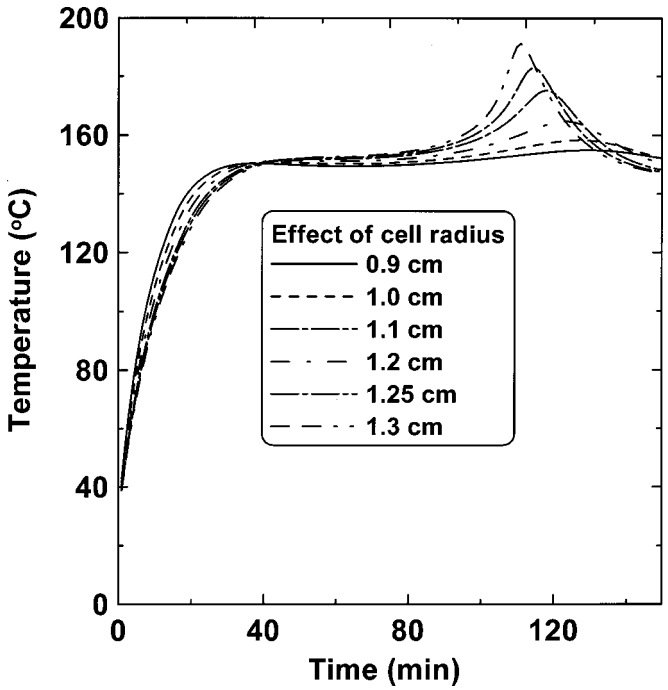

Figure 4. The effect of increasing cell radius on oven exposure tests for $LiCoO_2$/graphite chemistry (E-one/Moli type). A critical radius of 1.1 cm is found above which thermal runaway occurs in a 145°C oven.

ence between model and data to nearly zero. Even the interior temperature of the cylinder followed predictions very closely, and it was found that there is very little radial temperature gradient (about 1°C difference between center and surface) inside a metal cylinder in 18650 geometry when placed in an oven. These results give confidence in the numeric model of heat flow in a cylinder and encouraged building the final model of the lithium ion cell.

The small temperature gradient within the cylinder suggests that the solid cylinder can be treated as a lumped mass, having uniform temperature, with only heat flow at the surface being relevant. The Biot number for the cylinder was calculated to check this possibility. The Biot number is a dimensionless quantity that is a measure of the relative importance of heat flow within a body when compared to heat flow at the surface.[10] For the stainless steel cylinder, the Biot number is $Bi = h$ (volume/area)$/k = 0.00402$. Since this number is much less than one, the lumped mass approach is a good approximation for the solid stainless steel cylinder. The Biot number for an 18650 Li-ion battery was also checked. It is found to be 0.0179. This Biot number is also sufficiently low to warrant the use of a lumped mass or uniform temperature model. This was also included in the Visual C++ program. It was found that the predictions made by the two different methods were very close, but the uniform temperature model predicted a safe cell in an oven up to 3 K warmer than the full detail model. The uniform temperature model can then be used to obtain quick results (it is very much faster than the full detail model), but cases that are close to runaway should be checked with the full detail model.

Figure 2 shows some comparisons of model results and actual oven exposure tests on lithium-ion cells. From the figure it is clear that the model predicts the qualitative behavior of a cell in an oven exposure test very well. The initial warm-up to oven temperature is predicted nearly exactly for all oven temperatures. Also, the amount, and duration, of overshoot of the oven temperature is modeled very closely, and whether or not the cell will go to thermal runaway is also predicted accurately. The parameters used in the model were kept constant for each temperature. The parameters used are listed in Table I.

There are some deviations from model predictions in the oven test data. First, the exact time of thermal runaway is not predicted very well. This is due to the simple fact that the safety vent on the cell opens, electrolyte vapor is released, producing cooling by the Joule-Thompson effect in the actual cell that is unable to be included in the model. However, in the case of the cell that went to thermal runaway, it is clear from the steep slope of its temperature *vs.* time curve at the time of the venting that the cell would have exhibited runaway a few minutes sooner if not for the vent. This would bring the predicted time of runaway very close to the actual time of runaway.

The second major difference between the model and the actual tests is in the maximum temperature reached by the cell. The cell that went to thermal runaway reached a high temperature of approximately 700°C, while the model predicts a high temperature of only about 250°C. This discrepancy arises because the reaction model used for the cobalt cathode is incomplete. As shown in Ref. 2 and 3, there are three separate exotherms in the ARC and DSC experiments for $LiCoO_2$. However, only the first (lowest temperature) of these has been modeled and included in the simulations. In addition, there are further exothermic decompositions that take place above approximately 200°C, including the decomposition of the electrolyte itself, that have not been included in the model. Thus, the model can only predict the onset of thermal runaway (at the lowest temperatures) well. If the reaction kinetics of the remaining reactions were known and included in the model, then the model predictions would reproduce the high-temperature behavior more accurately.

Figure 3 tracks the progress of the two reactions at the anode and

Table II. Radii and electrode masses for Fig. 5.

Radius (cm)	Carbon mass (g)	$LiCoO_2$ mass (g)
0.90	6.0	12.0
1.00	7.4	14.8
1.10	9.0	18.0
1.20	10.7	21.3
1.25	11.6	23.1
1.30	12.5	25.0

the modeled reaction at the cathode for a 155°C oven test. This figure gives a very clear picture of what occurs inside a cell during an oven exposure test. First, at a temperature around 100°C, the metastable components of the SEI at the anode (as tracked by the variable x_f) decompose very rapidly. This provides a small temperature boost to the remaining reactants in the cell, which is enough to accelerate the reaction of the intercalated lithium at the anode (as tracked by the variable x_i). This reaction provides enough heat to overshoot the oven temperature and start the reactions at the cathode at a temperature of about 150°C (as tracked by the variable α). Using the reaction models developed previously,[1-3] α increases as the cathode/electrolyte reaction proceeds, while x_f and x_i decrease as the anode/electrolyte reaction proceeds. Both reactions continue to heat the cell until a temperature of about 175°C is reached at which time the reaction at the cathode accelerates, causing the remaining intercalated lithium at the anode to be used up much faster and the cell goes to thermal runaway. Even though the reactions at the anode take place at lower temperatures, they proceed relatively slowly until accelerated by the rapid reaction of the cathode. The cathode and intercalated lithium at the anode reacting at the same time are responsible for the extreme temperatures reached in thermal runaway. The parameters used in the model to generate this data set are again those listed in Table I.

Figure 4 shows the predicted effect of changing cell size. All the curves are calculated using the parameters that modeled the oven exposure data for a Moli 18650 cell (Fig. 2) listed in Table I. Each successive plot has the radius of the cell increased, and the amount of electrode material scaled up accordingly, as is shown in Table II. This reduces the surface area to volume ratio of the cell, making it

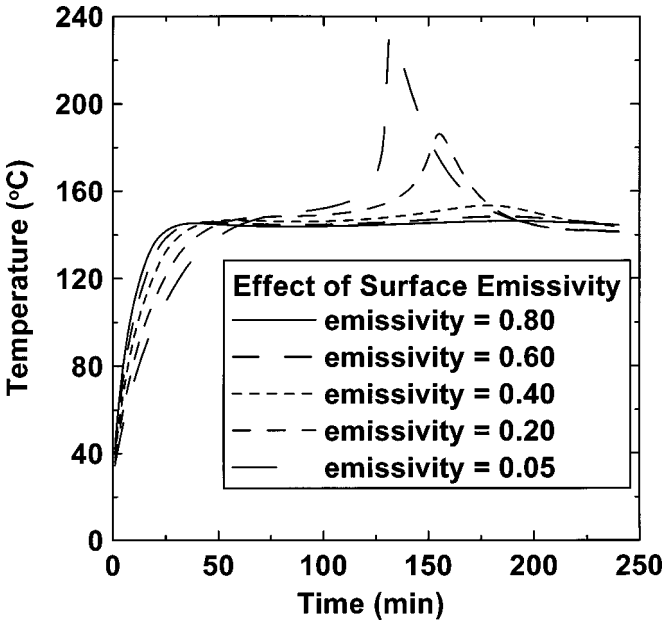

Figure 5. The effect of lowering surface emissivity on oven exposure tests. Below an emissivity of 0.40 the cell experiences thermal runaway in a 140°C oven.

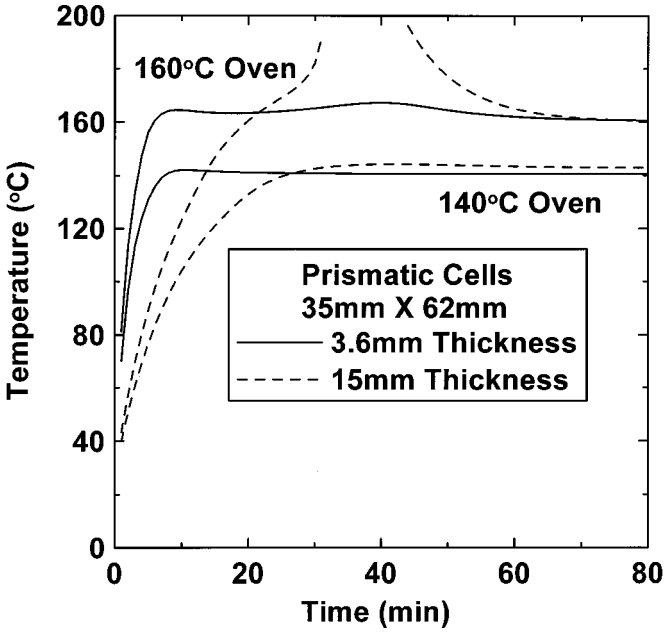

Figure 6. A comparison of oven exposure test predictions for $LiCoO_2$/graphite prismatic cells (4.2 V) of two thicknesses: (—) 3.6 and (– – –) 15 mm thick cell.

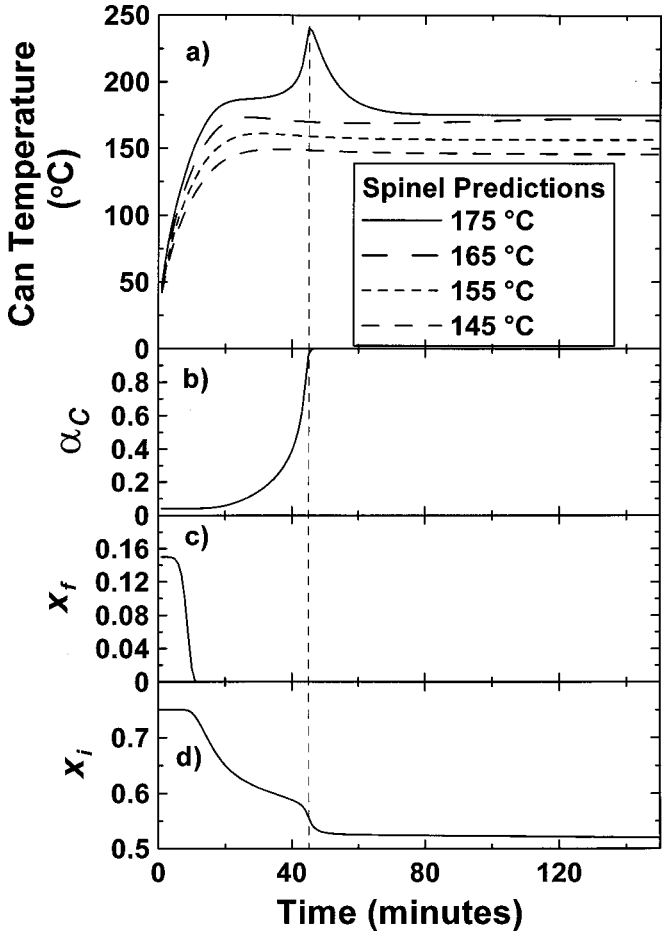

Figure 7. Model predictions for an 18650 cell with a less reactive cathode, such as spinel: (a) surface temperature of the cell, (b) fractional degree of conversion for the cathode, (c) decomposition of SEI layer, and (d) reaction of intercalated lithium at the anode; (b-d) correspond to 175°C predictions.

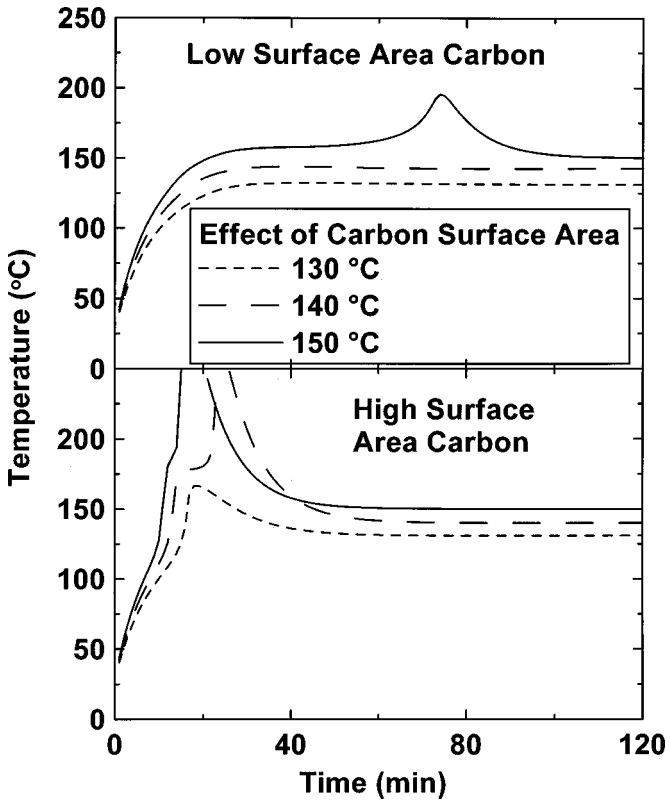

Figure 8. The effects of changing carbon surface area in $LiCoO_2$/graphite 18650 cells: (top) low surface area (bottom) high surface area carbon.

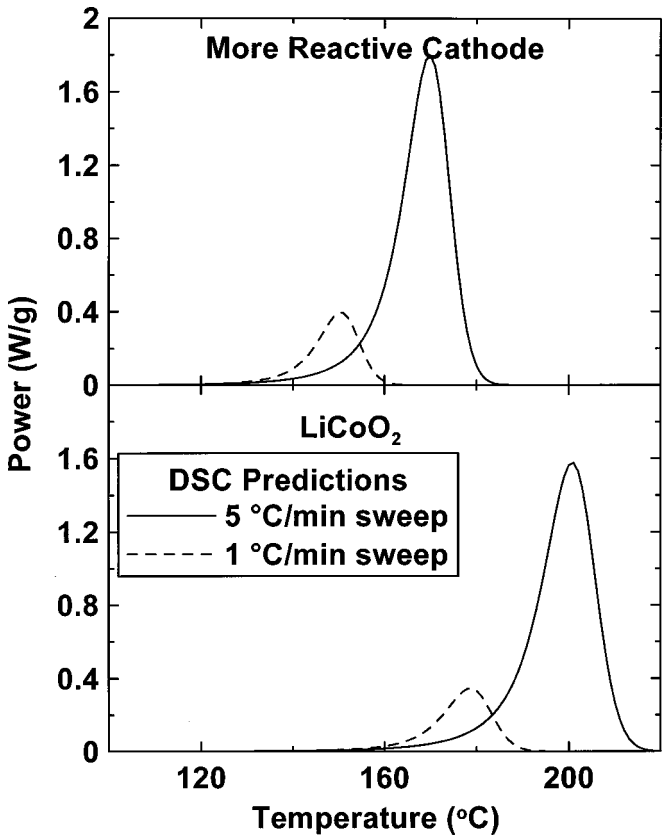

Figure 9. A comparison of calculated DSC traces for a $LiCoO_2$ cathode and a more reactive cathode: (top) more reactive cathode and (bottom) $LiCoO_2$; (—) 5°C/min and (– – –) 1°C/min sweep rate.

less efficient at dissipating internally generated heat. A critical radius of 1.1 cm was found above which thermal runaway was predicted in a 145°C oven (again, inclusion of the second and third cobalt exotherms as well as electrolyte decomposition would drive the runaway temperatures much higher). This indicates that the manufacturer would be able to increase the radius, and thereby the capacity, of its cell up to about 1.1 cm and still pass a 145°C oven exposure test. In the same way, a manufacturer could test the possibility of a capacity increase at an existing radius (by using denser or thicker electrodes) simply by increasing the mass of electrode material contained in the cell.

The heat-transfer coefficient is made up of two terms, one from convection and conduction, h_c, and the second from radiation, h_r.[8] The magnitude of the radiation term is directly proportional to the emissivity, ε, so the heat-transfer coefficient, h, is

$$h = h_c + \varepsilon h_r^{max}$$

For an 18650 cell in static air in a heated oven, we found $h_c = 0.000717$ W/cm^2 K and $h_r^{max} = 4\sigma T_W^3$ (T_W is oven temperature).[8] Figure 5 shows the effects of changing surface emissivity on the performance of an 18650 cell in the oven exposure test. The predictions were made with the standard parameter set of Table I. The only difference in the parameters for each data set is that the surface emissivity was varied as shown in the figure. These parameters predict the qualitative behavior of an E-one/Moli cell (surface emissivity 0.80) in a 140°C oven test very well (as demonstrated in Fig. 2). From Fig. 5, we see that as surface emissivity drops, the cell is less efficient at radiating/absorbing heat at the surface and so takes longer to heat up and also is more likely to go to thermal runaway. The model predicts the behavior described in Ref. 8 for cells with low-emissivity surfaces.

Figure 6 demonstrates the ability of thin prismatic cells to withstand high oven temperatures. Predictions were made for cells of two different thicknesses at two different temperatures. Cell sizes, capacities, and densities were based on those from Ref. 11. All parameters were the same for the cells except the thickness, and the amount of electrode material was scaled accordingly. The parameters used are shown in Table I. From the figure, it can be seen that both cells perform well in the 140°C oven test with little overshoot of the oven temperature. The largest difference between the two cells is that it takes the thicker cell longer to warm up, as expected. At the higher temperature, however, the thinner cell proves to be much safer. It overshoots by about 10°, but does not go to thermal runaway. The thicker cell cannot dissipate its internally generated heat fast enough and goes to thermal runaway. This behavior is very important for applications such as electric vehicles, where thin lithium ion or lithium ion polymer cells might be incorporated into the body panels. The manufacturer should be able to judge the safety performance of these body panel battery packs before actually assembling them.

Figure 7 shows some predictions for a cell with the same anode material as the E-one/Moli cells but with a less reactive cathode, perhaps spinel. To approximate the behavior of this less reactive cathode, the frequency factor for the cathode was reduced by a factor of five while the other parameters remained as shown in Table I. It should be noted that these parameters have not been fit to spinel data but are only meant as an approximation for illustration purposes. The top panel of the figure shows predictions for various oven temperatures, with runaway occurring at 175°C. This is similar to the behavior of E-one/Moli 18650 spinel cells in oven tests. The remaining panels track the changes in the reactions for the 175°C simulation. These graphs are very similar to Fig. 3, which showed predictions for a cobalt cell at 155°C.

Figure 8 shows the effects of different carbon surface areas. Here the parameters are the same as for the E-one/Moli cells in Table I,

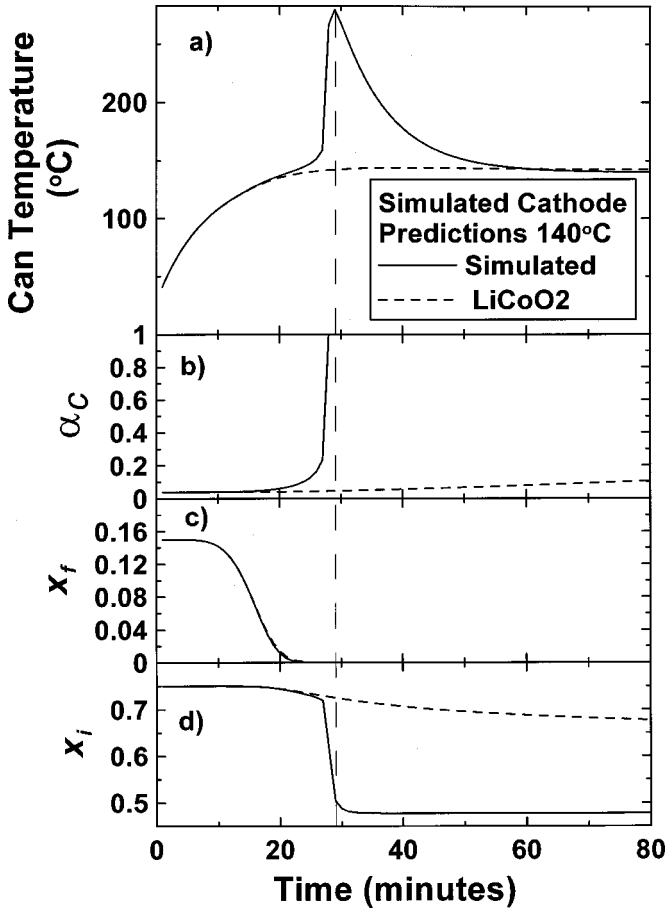

Figure 10. A comparison of oven exposure tests calculated for 18650 cells with $LiCoO_2$ and more reactive cathodes: (—) simulated more reactive cathode and (– – –) cobalt; (a) surface temperature of the cell, (b) fractional degree of conversion for the cathode, (c) decomposition of SEI layer, and (d) reaction of intercalated lithium at the anode.

except that H for the SEI has been increased by a factor of five, and x_{fo} has been increased to 0.25 from 0.15 for the case of a high surface area carbon. The increased surface area would cause a larger amount of SEI, which is what accounts for the increased H and x_{fo}. As shown in the figure, this increased amount of metastable SEI creates a lot more heat at the beginning of the test as the SEI decomposes. This provides an extra boost to the other reactions, which can cause thermal runaway in tests at much lower temperature. For the low surface area carbon, thermal runaway is not predicted until the oven temperature reaches 150°C. For high surface area carbons, thermal runaway is predicted at an oven temperature of 140°C. Clearly, lower surface area carbons are preferable to high surface area carbons for thermal stability of cells.

Figure 9 shows a comparison of predicted DSC curves for $LiCoO_2$ and another more reactive cathode material. The more reactive cathode was approximated by increasing the frequency factor for cobalt by a factor of ten. These predictions were not fit to any real data, but were meant only to illustrate the behavior of a more reactive cathode. The other parameters used for this figure are those of the standard set from Table I. As seen in the figure, the DSC trace for the simulated cathode is very similar to that for cobalt, except that it is shifted to the left about 25°C.

Figure 10 shows a comparison between a cobalt 18650 cell and an 18650 cell made from the simulated more reactive cathode at 140°C using the same parameters as for Fig. 9. Obviously the simulated cathode cell is unsafe at this temperature. The SEI in both the cobalt and simulated cells is used up very quickly, but the cobalt cell is not hot enough for the cathode to react and accelerate the second anode reaction. As a result, there is little self-heating of the cobalt cell and the reactions do not proceed very quickly at all. In the cell with the more reactive cathode the temperature is high enough for the cathode to react and the anode reaction is accelerated, causing thermal runaway. Again it should be noted that with inclusion of the second and third exotherms of the cathode, the temperature would be driven much higher and the anode reaction would go to completion.

Conclusion

It has been shown that it is possible to build an accurate model of oven exposure tests for Li-ion batteries using simple principles of heat flow and the technique in Ref. 1-3 for determining power functions of the electrode materials. This model has many uses for electrode developers. It can be used to determine the performance of cells made from new materials in abuse tests without actually producing test batches of cells. It would also allow for testing of new electrolytes or additives in the same way, although it is important to pay attention to the ratio of electrode material to electrolyte.[12] Also, the model can be used to test design changes to cells such as increases in radius or capacity. The model can also be used to predict the effects of changing to a more or less reactive cathode, changing to a higher or lower surface area carbon anode, and changing labels.

Acknowledgments

The authors thank NSERC and 3M Canada Co. for financial support under the Industrial Research Chair program and in the form of a NSERC postgraduate scholarship to one of us (T.D.H.). We thank E-One/Moli Energy (Canada), Ltd, for providing cells. Leif Christensen, Larry Krause, Jim Landucci, Ulrich von Sacken, Brian Way, Alf Wilson, and Jan Reimers participated in useful discussions about the model and its development.

Dalhousie University assisted in meeting the publication costs of this article.

References

1. M. N. Richard and J. R. Dahn, *J. Electrochem. Soc.*, **146**, 2078 (1999).
2. D. D. MacNeil, L. Christensen, J. Landucci, J. M. Paulsen, and J. R. Dahn, *J. Electrochem. Soc.*, **147**, 970 (2000).
3. D. D. MacNeil and J. R. Dahn, *J. Phys. Chem.*, Submitted (2000).
4. J. R. Dahn, D. D. MacNeil, and T. Hatchard, U.S. Pat. Appl., filed Dec 28, 1999.
5. H. Maleki, S. Al Hallaj, J. R. Selman, R. B. Dinwiddie, and H. Wang, *J. Electrochem. Soc.*, **146**, 947 (1999).
6. L. Song and J. W. Evans, *J. Electrochem. Soc.*, **146**, 869 (1999).
7. H. S. Carslaw and J. C. Jaeger, *Conduction of Heat in Solids*, 2nd ed., Oxford, London (1959).
8. T. D. Hatchard, D. D. MacNeil, D. A. Stevens, L. Christensen, and J. R. Dahn, *Electrochem. Solid-State Lett.*, **3**, 305 (2000).
9. *CRC Handbook of Chemistry and Physics*, 70th ed., CRC Press, Boca Raton, FL, (1989).
10. J. P. Holman, *Heat Transfer*, 8th ed., McGraw Hill, New York (1997).
11. N. Takami, M. Sekino, T. Ohsaki, M. Konda, M. Yamamoto, *Proceedings of the 10th International Meeting on Lithium Batteries*, Como, Italy, May 28-June 2, 2000.
12. D. D. MacNeil and J. R. Dahn, Paper 77 presented at The Electrochemical Society Meeting, Phoenix, AZ, Oct 22-27, 2000.